Bruno, Exposto, J. G. Pinto, Henrique Goncalves, Vítor Monteiro, Delfim Pedrosa, Carlos Couto, João L. Afonso

“Evaluation of a Shunt Active Power Filter with Energy Backup Capability”

Industrial Electronics Society, IECON 2013-39th Annual Conference of the IEEE

http://ieeexplore.ieee.org/document/6700113/

ISBN: 978-1-4799-0224-8

DOI 10.1109/IECON.2013.6700113

Bruno, Exposto, J. G.Pinto, Henrique Goncalves, Vítor Monteiro, Delfim Pedrosa, Carlos Couto, João L. Afonso, “Evaluation of a Shunt Active Power Filter with energy backup capability,” in Industrial Electronics Society, IECON 2013-39th Annual Conference of the IEEE, Vienna, Austria, 2013, pp. 5963–5968. DOI: 10.1109/IECON.2013.6700113, ISBN: 978-1-4799-0224-8

Evaluation of a Shunt Active Power Filter with Energy Backup Capability

Bruno Exposto, J. G. Pinto, Henrique Gonçalves, Vitor Monteiro, Delfim Pedrosa, Carlos Couto, João L. Afonso
Centro Algoritmi – University of Minho - Guimarães, Portugal
E-mails: {bruno.exposto, gabriel.pinto, henrique.goncalves, vitor.monteiro, delfim.pedrosa, carlos.couto, joao.l.afonso}@algoritmi.uminho.pt

***Abstract*— This paper presents a new Shunt Active Power Filter (SAPF) that is able to compensate current power quality problems and also to serve as energy backup to the loads in case of power outages. The paper describes the hardware topology, the control system of the SAPF, as well as the energy backup control scheme. Also it describes the power outage detection scheme to trigger the energy backup mode, as well as the grid synchronization after the power restoration. To assess the behavior of the SAPF when compensating power quality problems in transient and steady-state, and during the operation as energy backup system, several simulations were performed.**

Keywords—Energy Backup, Kalman Filter, Power Quality, p-q Theory, Shunt Active Power Filter, α-β PLL.

I. Introduction

Power quality problems have been a constant problem in electrical power grids along the years. Today exist different power electronics solutions to deal with power quality problems, which are classified as shunt conditioners [1][2], series conditioners [3], and an integrated approach of shunt and series conditioners known as Unified Power Quality Conditioners (UPQC) [4][5]. The Shunt Active Power Filter (SAPF) is connected in parallel with the electrical power grid to compensate current problems. Although the compensation characteristics of the SAPF are strictly related with the hardware topology and control algorithms, they were usually designed to mitigate the current harmonics, the current unbalances, the power factor and the neutral current upstream of the point of common coupling (PCC) in tree-phase four-wire installations. An electrical installation with a SAPF in operation absorbs from the power grid only the active power required by the loads, in a balanced way through the three phases, and with sinusoidal currents [6][7][8].

The SAPF integrates a three-phase power converter connected to the electrical power grid. In circumstances that do not involve compensation of power quality problems, this power converter can be used to perform other tasks, power outages are one of these situations. Power outages are known to cause high economic losses to the consumers, manly to some type of industries that have long chemical process that cannot be interrupted, at the risk of damaging the involved raw material and reagents [9]. Conventional backup equipment like Uninterruptible Power Supplies (UPS) and Diesel Generators can be used to compensate the voltage outages [10][11]. Notwithstanding the online UPS that operates continuously protecting the load against the most of the power quality problems, the offline UPS are idle for most of its useful lifetime. Considering that the power converters of a three phase offline UPS is very similar to the SAPF hardware, it would be advantageous combine the two functionalities in the same equipment.

In this paper is proposed a topology of SAPF that combines the functionalities of current compensation, when connected to the power grid, with the UPS functionalities, to feed the loads that are downstream in case of power outages. Therefore the equipment can be useful at full time, which translates in a shorter payback time. It must be referred that usually the apparent power of the SAPF is usually smaller than the apparent power of the loads, so to avoid the overdimensioning of the SAPF in case of power outages it can be used to feed only the priority loads. Otherwise it must be dimensioned for the total apparent power of the loads.

II. SAPF Topology and Control Algoritms

The SAPF has a topology composed by a three-phase four-wire shunt converter, with three IGBT legs and a split capacitor in the DC-link. This topology has the advantage of using less IGBTs when compared with the four leg topology. The disadvantage is the difficulty in the correct regulation of the DC-link voltages.

The power converter connects to the power grid trough three LCR passive output filter to eliminate the switching noise. In order to accomplish with the backup operating mode, the DC-link connects to the batteries through a reversible DC-DC power converter. This converter is used to adapt the batteries voltage to the SAPF DC-link voltage. This work is focused in the operation of the three-phase power converter as SAPF and as energy backup, and therefore this DC-DC converter is not described. The hardware topology of the SAPF with energy backup is presented in Fig.1.

The control of the SAPF is divided in several independent algorithms interacting in an integrated way. The main algorithms of the proposed digital controller consist in: the *p-q* Theory, a phase-locked loop (PLL), an output voltage and current control, a power grid outage detector and a resynchronizing procedure after power restoration.

A. p-q Theory

To compensate the power quality problems such as harmonic currents, current unbalances and low power factor it is necessary to dynamically calculate the compensation currents that must be produced by the SAPF. There are several techniques that can be used to perform this task, mainly divided in a frequency domain approach or time domain

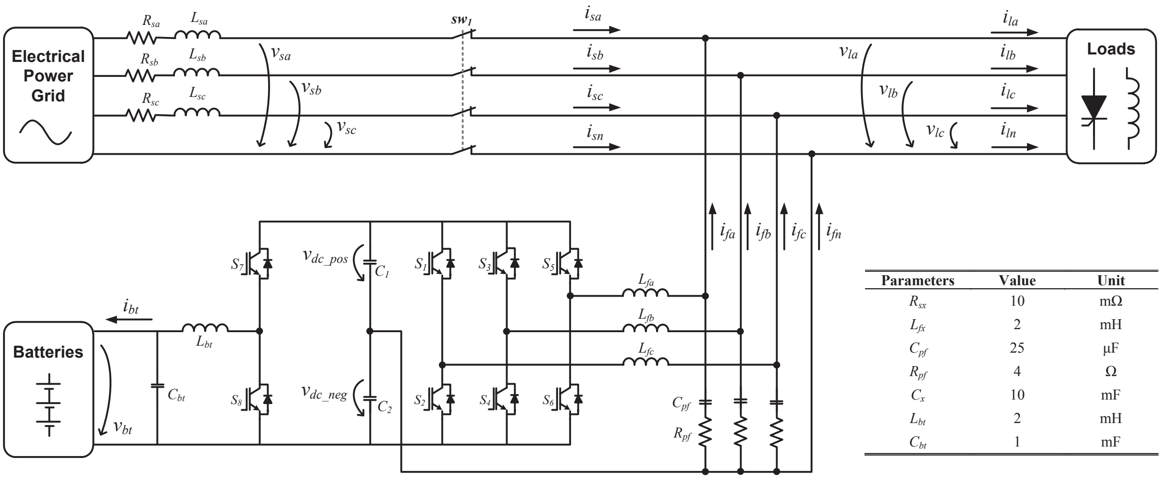

Parameters	Value	Unit
R_{sx}	10	mΩ
L_{fx}	2	mH
C_{pf}	25	μF
R_{pf}	4	Ω
C_x	10	mF
L_{bt}	2	mH
C_{bt}	1	mF

Fig. 1. Topology of the proposed Shunt Active Power Filter with energy backup.

approach [12]. Each one of those techniques has its advantages and disadvantages. The time domain approaches are known to require less processing capacity and to produce better transient response in case of load changes than the frequency domain approaches. On the other hand, frequency domain approaches usually allow the selection for individual harmonics compensation, which can be very useful in certain circumstances [13].

In this work it was chosen a time domain approach, the *p-q* Theory. This power theory, also known as the Theory of the Instantaneous Reactive Power, was proposed by Akagi et al. [14][15], and has been largely used in the control of power quality conditioners, providing an effective way to determine the compensating currents [16][17]. By the application of the *p-q* Theory the compensations currents are calculated to obtain a constant instantaneous power at the source. With sinusoidal power grid voltages this results in sinusoidal currents at the source. However with distorted power grid voltages, the currents at the source cannot be sinusoidal. There exists a little modification of the *p-q* Theory that instead of constant instantaneous power at source, results in sinusoidal currents at the source, even with distorted power grid voltages. This modification consists in using the positive sequence of the fundamental voltages instead of the real voltages [17][13]. Usually the power grid voltages do not present significant distortions, and therefore the application of the original *p-q* Theory and the modified ones produce very similar results. In this work it was implemented the sinusoidal source currents algorithm using a digital PLL in the α-β reference frame.

To determine the reference compensating currents the load currents are converted to the α-β reference frame through the Clarke transformation (1).

$$\begin{bmatrix} i_0 \\ i_\alpha \\ i_\beta \end{bmatrix} = \sqrt{\frac{2}{3}} \begin{bmatrix} 1/\sqrt{2} & 1/\sqrt{2} & 1/\sqrt{2} \\ 1 & -1/2 & -1/2 \\ 0 & \sqrt{3}/2 & -\sqrt{3}/2 \end{bmatrix} \begin{bmatrix} i_{la} \\ i_{lb} \\ i_{lc} \end{bmatrix} \quad (1)$$

The same should be done with the system voltages if we want to implement the constant instantaneous power at the source algorithm. In this work was implemented the sinusoidal source currents algorithm, the positive sequence of the system voltages is used, and is obtained directly in the α-β reference frame using the PLL signals. Having i_α, i_β, v_{α_pll} and v_{β_pll} are then calculated the instantaneous real power p and the instantaneous imaginary power q through (2).

$$\begin{bmatrix} p \\ q \end{bmatrix} = \begin{bmatrix} v_{\alpha\_pll} & -v_{\beta\_pll} \\ v_{\beta\_pll} & v_{\alpha\_pll} \end{bmatrix} \begin{bmatrix} i_\alpha \\ i_\beta \end{bmatrix} \quad (2)$$

After determining p, is applied a sliding window average with 640 positions (which corresponds to one 50 Hz grid cycle, considering a sampling frequency of 32 kHz), and its obtained the mean value of the instantaneous power, $\bar{p}$. With the value of $\bar{p}$ it is possible to determinate the oscillating part of the instantaneous real power, $\tilde{p}$:

$$\tilde{p}=p-\bar{p}\ . \quad (3)$$

The next step is the calculation of the compensating currents in the α-β reference frame applying (4):

$$\begin{bmatrix} i_{c\alpha} \\ i_{c\beta} \end{bmatrix} = \frac{1}{{v_{\alpha pll}}^2+{v_{\beta pll}}^2} \begin{bmatrix} v_{\alpha\_pll} & -v_{\beta\_pll} \\ v_{\beta\_pll} & v_{\alpha\_pll} \end{bmatrix} \begin{bmatrix} \tilde{p} \\ q \end{bmatrix} \quad (4)$$

The compensation currents are then translated to the *a-b-c* reference frame applying (6). Being this a three-phase four wire SAPF, the compensated components in the system are: q, $\tilde{p}$ and i_0, and consequently:

$$i_{c0}=i_0 \quad (5)$$

$$\begin{bmatrix} i_{ca} \\ i_{cb} \\ i_{cc} \end{bmatrix} = \sqrt{\frac{2}{3}} \begin{bmatrix} 1/\sqrt{2} & 1 & 0 \\ 1/\sqrt{2} & -1/2 & \sqrt{3}/2 \\ 1/\sqrt{2} & -1/2 & -\sqrt{3}/2 \end{bmatrix} \begin{bmatrix} i_{c0} \\ i_{c\alpha} \\ i_{c\beta} \end{bmatrix} \quad (6)$$

The regulation of the DC-link capacitors voltage is done independently using two PI controllers, one per capacitor.

$$p_{reg\_x}=k_p\left(v_{dc\_x}{}^{*}-v_{dc\_x}\right)+\frac{1}{k_i}\int\left(v_{dc\_x}{}^{*}-v_{dc\_x}\right) \quad (6)$$

After that is calculated using p_{reg_x} and the reference voltages, obtained though the PLL in the *a-b-c* reference frame, the regulating currents. The DC-link regulation is done taking in account the signal of v_{x_pll} as can be seen in (7). In this case the topology of the inverter is with split capacitor, so in the positive semi-cycle of the grid voltages, is done the regulation of the top capacitor and in the negative semi-cycle is done the regulation of the bottom capacitor.

$$i_{reg\_x}=\begin{cases} p_{reg\_pos}\dfrac{v_{x\_pll}}{v_{a\_pll}^2+v_{b\_pll}^2+v_{c\_pll}^2}, v_{x\_pll}\geq 0 \\ p_{reg\_neg}\dfrac{v_{x\_pll}}{v_{a\_pll}^2+v_{b\_pll}^2+v_{c\_pll}^2}, v_{x\_pll}<0 \end{cases} \quad (7)$$

The reference currents send to the modulator are i_{cx} - i_{reg_x}. This is done to all the phases of the system. This strategy is similar to what is done in [18]. In Fig. 2 can be seen all the blocks and respective connections.

B. Three-Phase PLL

The implemented three-phase PLL was proposed by Aredes et al. [19]. This PLL has several advantages, namely the fact of being simple to implement and robust. In Fig. 3 is possible to see a diagram of the PLL. In this work the PLL is used not only to determine the positive sequence of the system voltages and implement the sinusoidal currents at source algorithm, but also to generate the reference voltages when a power outage is occurring. To perform this task, the PLL was modified and was added the nominal frequency of the voltages (ω_0=100π rads/s), before the integrator (Fig. 3). This enables the generation of the reference voltages to the SAPF, even when a power outage is occurring.

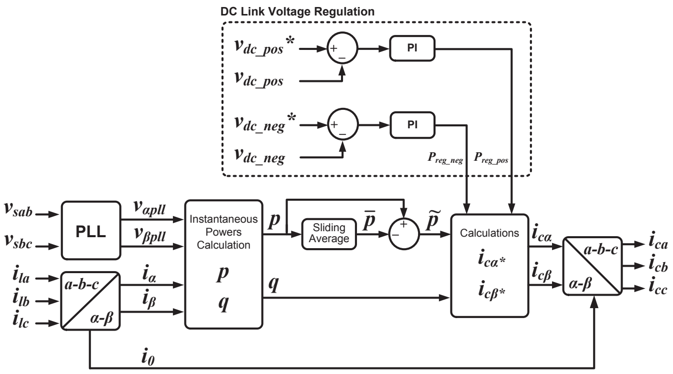

Fig. 2. Implemented *p-q* Theory control scheme.

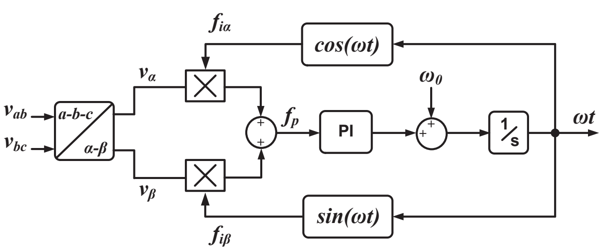

Fig. 3. Diagram of the implemented *a-β* PLL.

The other tasks that imply the use of the PLL, are the synchronization of the SAPF voltages when occurs the grid voltage restoration and the detection of when is complete the synchronization between the grid voltages and the inverter voltages.

C. Current and Voltage Control and Modulation Technique

The current control in the SAPF is done using three PI controllers, one per phase. The implemented modulation technique is bipolar pulse-width modulation. This modulation technique has several advantages, mainly the fact that guarantees fixed switching frequency and has a low final THD [20].

The voltage control consists in directly compare the reference voltages with the triangular carrier and then use the result of the comparison in the power switches. In both cases, the switching frequency was fixed in 20 kHz.

III. Energy Backup Control Scheme

The energy backup control algorithm is composed by several parts. In a normal situation it is working as a SAPF compensator. At the same time the grid fault detector is monitoring the phase voltages. If the RMS value of at least one of them is lower than 80% of the nominal voltage (in this work the nominal voltage is defined as 230 V), the control acts to isolate the loads and the SAPF from the power grid (forming an island). Then the control of the SAPF passes from current control to voltage control. As aforementioned, the implemented PLL provides the reference voltages to be produced. In this moment, the SAPF is acting as an energy backup feeding the loads downstream of the PCC. It must be referred that, although the SAPF and the loads are isolated from the grid, the grid voltages are still being monitored by the grid fault detector, to detect the power restoration.

When is detected that the RMS value of the voltages in all the phases is above 80% of the nominal value), the SAPF produced voltages start to be synchronized with the grid voltages. This is done using the implemented PLL. After the resynchronization the SAPF resumes its normal operation. In Fig. 4 is possible to see a diagram with all of these steps.

A. Grid Fault Detection Scheme

In a situation where exists a sag higher than 20% of the nominal voltage, or an power outage, the fault detection algorithm is responsible for detect that situation, activate the energy backup of the SAPF and give the necessary signal to the other parts of the control that will isolate the loads and the SAPF from the power grid, or eventually, if it is contemplated, to separate the critical loads from the other loads, feeding them from the SAPF.

There are in the literature several algorithms that can perform this task with more or less effectiveness and more or less processing time. In Moschitta, et al. [21] and Amarís et al. [22] the authors make a comparison of several sag and power outage detection methods. In both of the two papers is showed that a Kalman filter can be used with success in the detection of sags and power outages. Although that the authors propose and discuss other methods, the Kalman filter method has a good

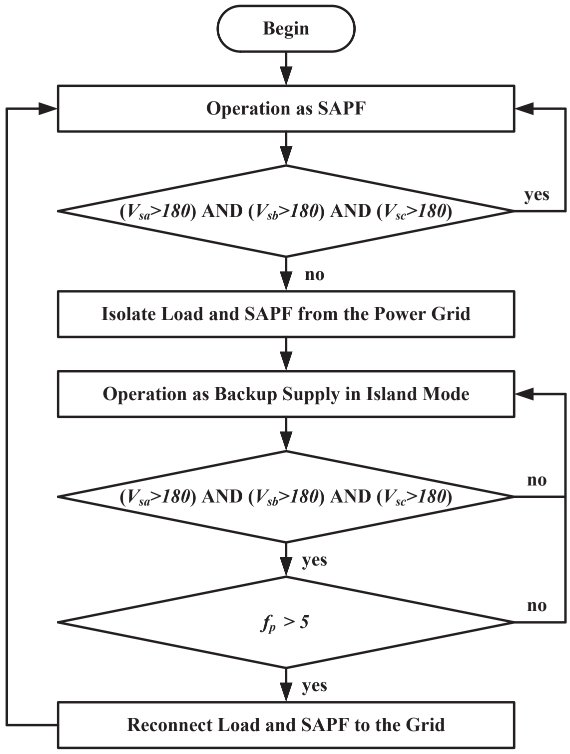

Fig. 4. Shunt Active Power Filter operation diagram.

performance, and has the advantages being simple to implement, fast and efficient in terms of processing time. With this in mind, in this work were used three Kalman filters (one per phase) to determine the grid power outages and restorations.

To implement the Kalman filter is necessary the model of the system voltage (8), and its quadrature (9) [21][22].

$$s(t)=A\sin(2\pi f_0 t) \tag{8}$$

$$q(t)=A\cos(2\pi f_0 t) \tag{9}$$

If the signal is sampled with a defined sampling frequency we can obtain a discretized model of the system voltages (10)(11).

$$s[n]=s(nT_s) \tag{10}$$

$$q[n]=q(nT_s) \tag{11}$$

Considering these equations is possible to establish the following state model:

$$x[n]=Sx[n\text{-}1]+v[n\text{-}1] \tag{12}$$

In which,

$$S=\begin{bmatrix}\cos(2\pi f_0 T_s) & \sin(2\pi f_0 T_s)\\ -\sin(2\pi f_0 T_s) & \cos(2\pi f_0 T_s)\end{bmatrix} \tag{13}$$

Given this, the estimation or the RMS of the voltages is preceded by several steps. The first one is the calculation of the Kalman gain (14).

$$K[n]=\hat{P}[n]H^T(H\hat{P}[n]H^T+R[n])^{-1} \tag{14}$$

The next step is the update of the state estimation using the Kalman gain:

$$x[n]=\hat{x}[n]+K[n](z[n]\text{-}H\hat{x}[n]) \tag{15}$$

After this, the next step is the calculation of the error covariance.

$$P[n]=(I\text{-}K[n]H\hat{P}[n]) \tag{16}$$

Being:

$$H=[1 \quad 0] \tag{17}$$

Finally, having all the ulterior parameters is possible to calculate the future values of the state estimation ($\hat{x}[n+1]$) and error covariance ($\hat{P}[n+1]$).

$$\hat{x}[n+1]=Sx[n]+w[n] \tag{18}$$

$$\hat{P}[n+1]=SP[n]S^T+Q[n] \tag{19}$$

The estimation of the RMS value of the voltage signal is given by (20).

$$\hat{A}_{RMS}=\sqrt{\frac{\hat{s}[n]^2+\hat{q}[n]^2}{2}} \tag{20}$$

B. Grid Syncronization After Grid Power Restoration

During a power outage, the SAPF and the loads are isolated from the power grid, nevertheless the voltages in the three phases of the power grid is always monitored. If is detected that RMS value of all the voltages is above 80% of the nominal RMS value, the control acts to reconnect the SAPF and the loads to grid and resume the normal SAPF operation. This reconnection implies that the load voltages supplied by the SAPF are synchronized with the power grid voltages. As was said before, the PLL generates the reference voltages during the power outage. When happens the restoration, the PLL will start to do the synchronization between the reference voltages and the power grid voltages. This takes some time, because in this situation the synchronization time is extended to three grid cycles. Due to this synchronization of the PLL with the power grid voltages and keeping in mind that the PLL is generating the reference voltages to the SAPF and the generated voltages will synchronize with the power grid voltages. After sometime when the synchronization is complete, the SAPF and the loads are reconnected to the power grid. To detect if the grid voltages and the SAPF voltages are synchronized, the parameter f_p of the PLL is monitored. When the value of f_p is lower than 5, it is considered that the synchronization is complete.

IV. Simulation Results

With the simulation models developed, it is possible to test the behavior of the SAPF during different conditions of operation, both in steady-state and transient state. During normal conditions of operation the SAPF compensates the current harmonics, the current unbalances and the power factor of the loads, as shown in Fig. 5. In Fig. 5 (a) are shown the source voltages (v_{sa}, v_{sb}, v_{sc}), in Fig. 5 (b) the source currents (i_{sa}, i_{sb}, i_{sc}, i_{sn}), in Fig. 5 (c) the load voltages (v_{la}, v_{lb}, v_{lc}), in Fig. 5 (d) the load currents (i_{la}, i_{lb}, i_{lc}, i_{ln}), and in Fig. 5 (e) the compensation currents (i_{fa}, i_{fb}, i_{fc}, i_{fn}). It can be seen that by the action of the SAPF the currents in the source become sinusoidal, whereas the currents in the loads are distorted and unbalanced.

When a power outage occurs, it is detected by the control algorithm and the SAPF starts to operate as energy backup system. In Fig. 6 is shown the operation of the SAPF during a power outage. In Fig. 6 (a) are shown the source voltages (v_{sa}, v_{sb}, v_{sc}), in Fig. 6 (b) the source currents (i_{sa}, i_{sb}, i_{sc}, i_{sn}), in Fig. 6 (c) the load voltages (v_{la}, v_{lb}, v_{lc}), in Fig. 6 (d) the load currents (i_{la}, i_{lb}, i_{lc}, i_{ln}), and in Fig. 6 (e) the compensation currents (i_{fa}, i_{fb}, i_{fc}, i_{fn}). It can be seen that when the source voltage fails, the SAPF immediately starts to operate in the voltage operating mode, and therefore the loads voltages and currents are not interrupted.

After a power outage, when the power is restored, the control algorithm detects the source voltages and starts to operate as SAPF again. In Fig. 7 is shown the operation of the SAPF during a power restoration. In Fig. 7 (a) are shown the source voltages (v_{sa}, v_{sb}, v_{sc}), in Fig. 7 (b) the source currents (i_{sa}, i_{sb}, i_{sc}, i_{sn}), in Fig. 7 (c) the load voltages (v_{la}, v_{lb}, v_{lc}), in Fig. 7 (d) the load currents (i_{la}, i_{lb}, i_{lc}, i_{ln}), and in Fig. 7 (e) the compensation currents (i_{fa}, i_{fb}, i_{fc}, i_{fn}). In the presented simulation results, the transition from the island mode to the grid connected mode is done in one grid cycle, causing a frequency variation in the load voltages. This is intentionally performed to show the resynchronizing algorithm in operation. In practice, the frequency variation during the transaction can be significantly minimalized by increasing the resynchronizing time. After the transition, the SAPF starts to compensate de load currents again. In Fig. 8 are shown the control variables involved in resynchronization process. In Fig. 8 (a) is shown the source voltage (v_{sa}) and the PLL reference signal (v_{α_pll}), and in Fig. 8 (b) is shown the PLL reference signal (f_p) that corresponds to the phase difference between v_{sa} and v_{α_pll}.

V. Conclusions

This paper presents a Shunt Active Power Filter (SAPF) that is able to compensate power quality problems and that also serves as energy backup system during power outages.

First, the simulation results indicate that the SAPF can successfully compensate the current harmonics, the current unbalances and the power factor. The *p-q* Theory used in the digital controller successfully identifies the current components that must be compensated by the SAPF. The simulation results also show that the SAPF can be used as energy backup system in case of a power outage. The power outage detection scheme performs correctly, but further tests are needed, namely with different loads and power outage conditions. The synchronization mechanism also performs correctly.

For future work it will be implemented an experimental prototype to assess its real performance and validate the simulation results.

Acknowledgment

This work is financed by FEDER Funds, through the Operational Programme for Competitiveness Factors – COMPETE, and by National Funds through FCT – Foundation for Science and Technology of Portugal, under the projects PTDC/EEA-EEL/104569/2008 and FCOMP-01-0124-FEDER-022674.

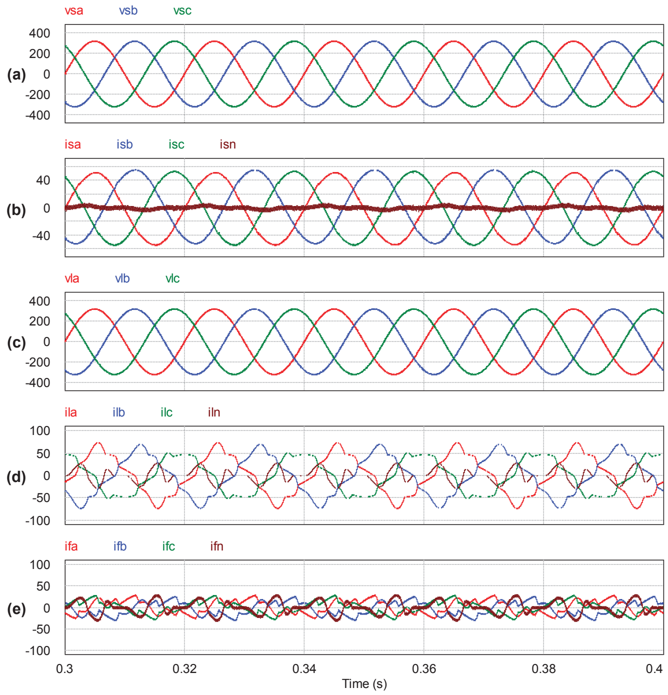

Fig. 5. Simulation results of the SAPF compensating the distortion of the currents in the loads: (a) Source voltages (v_{sa}, v_{sb}, v_{sc}); (b) Source currents (i_{sa}, i_{sb}, i_{sc}, i_{sn}); (c) Load voltages (v_{la}, v_{lb}, v_{lc}); (d) Load currents (i_{la}, i_{lb}, i_{lc}, i_{ln}); (e) Compensation currents (i_{fa}, i_{fb}, i_{fc}, i_{fn}).

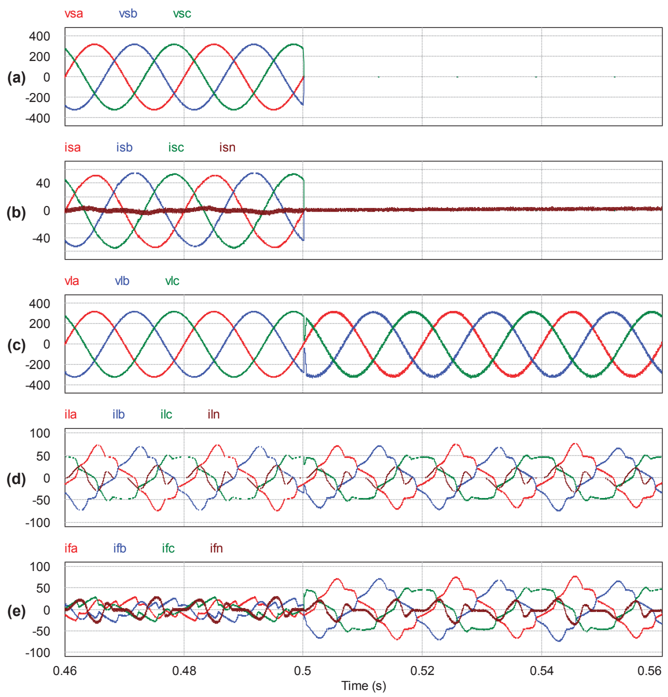

Fig. 6. Simulation results of the SAPF during a power outage: (a) Source voltages (v_{sa}, v_{sb}, v_{sc}); (b) Source currents (i_{sa}, i_{sb}, i_{sc}, i_{sn}); (c) Load voltages (v_{la}, v_{lb}, v_{lc}); (d) Load currents (i_{la}, i_{lb}, i_{lc}, i_{ln}); (e) Compensation currents (i_{fa}, i_{fb}, i_{fc}, i_{fn}).

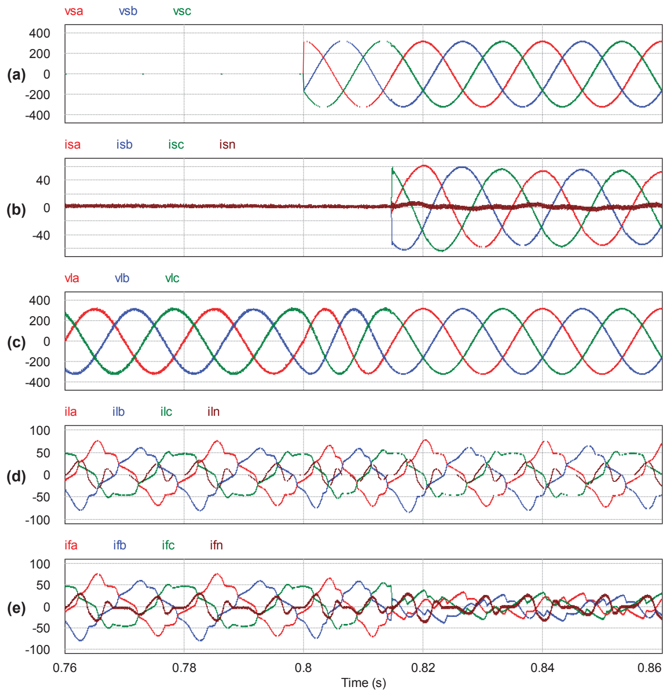

Fig. 7. Simulation results of the SAPF during a power restoring: (a) Source voltages (v_{sa}, v_{sb}, v_{sc}); (b) Source currents (i_{sa}, i_{sb}, i_{sc}, i_{sn}); (c) Load voltages (v_{la}, v_{lb}, v_{lc}); (d) Load currents (i_{la}, i_{lb}, i_{lc}, i_{ln}); (e) Compensation currents (i_{fa}, i_{fb}, i_{fc}, i_{fn}).

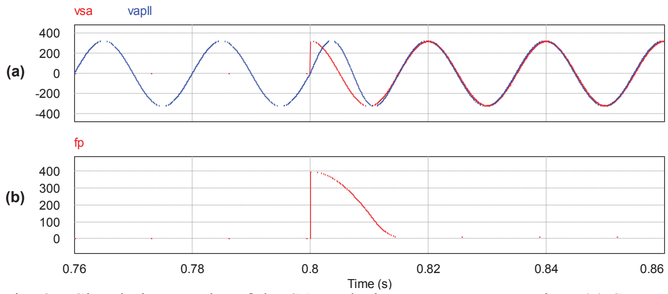

Fig. 8. Simulation results of the SAPF during a power restoration: (a) Source voltage in phase *a* (v_{sa}) and PLL reference signal (v_{a_pll}); (b) Phase diference between the source voltage in phase *a* and the PLL reference signal (f_p).

REFERENCES

[1] B. Singh, K. Al-Haddad, and A. Chandra, "A review of active filters for power quality improvement," *Industrial Electronics, IEEE Transactions on*, vol. 46, no. 5, pp. 960–971, 1999.

[2] H. Akagi, "New trends in active filters for power conditioning," *Industry Applications, IEEE Transactions on*, vol. 32, no. 6, pp. 1312–1322, 1996.

[3] A. Javadi, N. Geiss, H. F. Blanchette, and K. Al-Haddad, "Series active conditionners for reliable Smart grid: A comprehensive review," in *IECON 2012-38th Annual Conference on IEEE Industrial Electronics Society*, 2012, pp. 6320–6327.

[4] V. Khadkikar, "Enhancing electric power quality using UPQC: A comprehensive overview," *Power Electronics, IEEE Transactions on*, vol. 27, no. 5, pp. 2284–2297, 2012.

[5] H. Fujita and H. Akagi, "The unified power quality conditioner: the integration of series and shunt-active filters," *Power Electronics, IEEE Transactions on*, vol. 13, no. 2, pp. 315–322, 1998.

[6] J. Pinto, B. Exposto, V. Monteiro, L. F. Monteiro, C. Couto, and J. L. Afonso, "Comparison of Current-Source and Voltage-Source Shunt Active Power Filters for Harmonic Compensation and Reactive Power Control," in *IECON 2012-38th Annual Conference on IEEE Industrial Electronics Society*, 2012, pp. 5161–5166.

[7] B. Exposto, H. Gonçalves, and J. L. and Afonso, "Sequence Detectors for Highly Distorted and Unbalanced Systems," - *Electrical Power Quality and Utilization Conference, Proceedings IEEE EPQU 2011*, pp. 1 –6, 2011.

[8] B. Exposto, H. Gonçalves, J. Pinto, J. L. Afonso, and C. Couto, "Three Phase Four Wire Shunt Active Power Filter from Theory to Industrial Facility Tests," in *Electrical Power Quality and Utilisation (EPQU), 2011 11th International Conference on*, 2011, pp. 1–5.

[9] W. E. Brumsickle, R. S. Schneider, G. A. Luckjiff, D. M. Divan, and M. F. McGranaghan, "Dynamic sag correctors: cost-effective industrial power line conditioning," *Industry Applications, IEEE Transactions on*, vol. 37, no. 1, pp. 212–217, 2001.

[10] D. Van Hertem, M. Didden, J. Driesen, and R. Belmans, "Optimal mitigation of voltage dips and interruptions," in *Proc. IEEE Young Researchers Symposium in Electrical Power Engineering, Delft, The Netherlands*, 2004.

[11] D. Van Hertem, M. Didden, J. Driesen, and R. Belmans, "Choosing the correct mitigation method against voltage dips and interruptions: A customer-based approach," *Power Delivery, IEEE Transactions on*, vol. 22, no. 1, pp. 331–339, 2007.

[12] D. Marshall, J. Van Wyk, F. Venter, L. Malesani, and A. Zuccato, "A comparative evaluation of power theories," in *Harmonics in Power Systems., ICHPS V International Conference on*, 1992, pp. 142–150.

[13] L. F. C. Monteiro, J. L. Afonso, J. G. Pinto, E. Watanabe, M. Aredes, and H. Akagi, "Compensation algorithms based on the pq and CPC theories for switching compensators in micro-grids," in *Power Electronics Conference, 2009. COBEP'09. Brazilian*, 2009, pp. 32–40.

[14] H. Akagi, Y. Kanazawa, and A. Nabae, "Generalized theory of the instantaneous reactive power in three-phase circuits," in *IPEC*, vol. 83, 1983, pp. 1375–1386.

[15] H. Akagi, Y. Kanazawa, and A. Nabae, "Instantaneous reactive power compensators comprising switching devices without energy storage components," *Industry Applications, IEEE Transactions on*, no. 3, pp. 625–630, 1984.

[16] H. Akagi, E. H. Watanabe, and M. Aredes, *Instantaneous power theory and applications to power conditioning*, vol. 31. Wiley-IEEE Press, 2007.

[17] J. L. Afonso, C. Couto, and J. S. Martins, "Active filters with control based on the pq theory," *IEEE Industrial Electronics Society Newsletter*, vol. 47, no. 3, pp. 5–10, 2000.

[18] F. Ferreira, L. Monteiro, J. L. Afonso, and C. Couto, "A control strategy for a three-phase four-wire shunt active filter," in *Industrial Electronics. IECON 2008. 34th Annual Conference of IEEE*, 2008, pp. 411–416.

[19] L. B. Rolim, D. R. da Costa, and M. Aredes, "Analysis and software implementation of a robust synchronizing PLL circuit based on the pq theory," *Industrial Electronics, IEEE Transactions on*, vol. 53, no. 6, pp. 1919–1926, 2006.

[20] J. W. Dixon, S. Tepper, and L. Moran, "Analysis and evaluation of different modulation techniques for active power filters," in *Applied Power Electronics Conference and Exposition, 1994. APEC'94. Conference Proceedings 1994., Ninth Annual*, 1994, pp. 894–900.

[21] A. Moschitta, P. Carbone, and C. Muscas, "Performance comparison of advanced techniques for voltage dip detection," *Instrumentation and Measurement, IEEE Transactions on*, vol. 61, no. 5, pp. 1494–1502, 2012.

[22] H. Amaris et al., "Computation of voltage sag initiation with Fourier based algorithm, Kalman filter and wavelets," in *PowerTech, 2009 IEEE Bucharest*, 2009, pp. 1–6.